Proceedings of the 7th International Conference on Gas Hydrates (ICGH 2011),
Edinburgh, Scotland, United Kingdom, July 17-21, 2011.

CO_2 INJECTION INTO SUBMARINE SEDIMENTS: DISTURBING CH_4 HYDRATES

Nikolaus K. Bigalke [*]
Christian Deusner
Elke Kossel
Matthias Haeckel
Leibniz Institute of Marine Sciences (IFM-GEOMAR)
24148 Kiel
GERMANY

ABSTRACT

The production of natural gas via injection of fossil-fuel derived CO_2 into submarine gas hydrate reservoirs can be an example of tapping a hydrocarbon energy source in a CO_2-neutral manner. However, the industrial application of this method is technically challenging. Thus, prior to feasibility testing in the field, multi-scale laboratory experiments and adapted reaction-modeling are needed. To this end, high-pressure flow-through reactors of 15 and 2000 mL sample volume were constructed and tested. Process parameters (*P*, *T*, *Q*, fluid composition) are defined by a fluid supply and conditioning unit to enable simulation of natural fluid-flow scenarios for a broad range of sedimentary settings. Additional Raman- and NMR- spectroscopy aid in identifying the most efficient pathway for CH_4 extraction from hydrates via CO_2 injection on both microscopic and macroscopic level. In this study we present experimental set-up and design of the high-pressure flow-through reactors as well as CH_4 yields from CH_4-hydrate decomposition experiments using CO_2-rich brines and pure liquefied CO_2.

Keywords: CO_2 injection, hydrate conversion, CH_4 extraction, hydrate-bearing sediments

[*] Corresponding author: Phone: +49(0)431 600 1410, Fax: +49(0)431 600 1400, E-mail: nbigalke@ifm-geomar.de

INTRODUCTION

The rising awareness of adverse impacts ascribed to the continued anthropogenic input of CO_2 into the exchangeable carbon reservoir has fueled efforts to identify strategies helping to minimize CO_2 emissions. One of the means presently discussed is based on the replacement of CH_4 by CO_2 in gas hydrates (i.e. ”hydrate conversion”). The injection of CO_2 into gas hydrate-bearing marine sediments could fulfill the double duty of producing clean-burning hydrocarbons, chiefly CH_4, whilst permanently disposing of one of the most notorious greenhouse gases as immobile CO_2 hydrate.

Assessing the technical feasibility of industry-scale implementation of this prospect in the field requires reliable model calculations simulating geological and geochemical processes following CO_2 injection. The accuracy of these simulations largely depends on input parameters characterizing reservoir conditions and identifying mechanisms and rates of process parameters. Methods and tools necessary to obtain such information include classical field studies but also experimental laboratories capable of establishing environments characterized as extreme with regard to pressure, temperature as well as sediment and fluid composition. A large number of studies have emerged over the recent years [1-9], each of them using task-specific experimental platforms suitable to address hydrate conversion from a particular perspective (thermodynamics, kinetics and/or fluid dynamics). However, a persisting shortcoming is the dearth of experimental studies integrating multiple perspectives in a single approach. Moreover, most experimental efforts to date neglect hydraulic effects of sediment properties such as porosity and permeability on hydrate conversion efficiency. While expanding the mechanistic understanding of hydrate conversion, the aforementioned, segregated approaches may not suffice to elucidate the response of dynamic, near-natural systems to CO_2 injection. Apart from delivering the extreme environmental conditions specified above, an integrated approach therefore requires experimental tools allowing on-line monitoring and control of multiple process parameters while hydrate conversion is in progress.

Most recently, Schicks et al. [10] introduced a 425 L pressure vessel used to form and decompose CH_4 hydrate in sandy sediments at simulated reservoir conditions. Hydrate dissociation was achieved by thermal stimulation via electric heating to mimic catalytic oxidation of the hydrate-fixed CH_4. First test runs not only demonstrate the general viability of the method but also reveal the complex response of the reservoir due to heterogeneous heat transport in the sediment.

The approach followed in this study proposes pressure laboratories with experiments in which hydrate-bearing sediments are percolated by reactive fluids as means to elucidate geochemical and –mechanical phenomena taking place after CO_2 injection into sandy marine sediments. Two different experimental tools are presented. The first is used to quantify CH_4 yields from CH_4-hydrate decomposition experiments using CO_2-rich brines, pure liquefied, supercritical as well as gaseous CO_2. Quantification of CH_4 yields is based on mass balancing fluids supplied to and extracted from the experimental domain. The second set up permits additional high-resolution magnetic resonance imaging (MRI) of the experimental domain while CH_4 hydrates decompose in the fluid percolating through sediment. Presentation of the results is strongly focused on demonstrating system functionality and feasibility for the experimental purposes. We will also exemplify process complications which need to be considered in both future experimentation and process development in a more general sense.

EXPERIMENTAL SYSTEMS AND PROCEDURES

System principle of flow-through experiments

The high-pressure flow-through system is designed to be operated as a one or two-stage system. In the sample vessel hydrate sediment samples can be prepared in several defined ways (see Section “CH_4-hydrate preparation”). The sample vessels are equipped with cooling jackets and temperature controls suitable for hydrate experimentation. Fluid preparation is achieved by mixing of defined volumes of water or seawater and gas at the respective pressure conditions. Pressurized gases are delivered into the system independently from reservoir bottles or by a high-pressure syringe pump 260D (TELEDYNE ISCO, Lincoln, USA). All incubation fluids are delivered to the sample vessel under controlled *P*-/*T*-conditions with defined volume flow rates. Upstream and downstream of the sample vessel different sensors are installed for online process monitoring of pressure, temperature, conductivity

and gas concentrations or gas partial pressures (see Section “Sensor systems, process monitoring and analytical methods”). Sampling ports are installed to collect fluid samples for water and gas analysis. The system also includes a possibility to collect the bulk fluids downstream of the reactor. A basic flow scheme is shown in Figure 1.

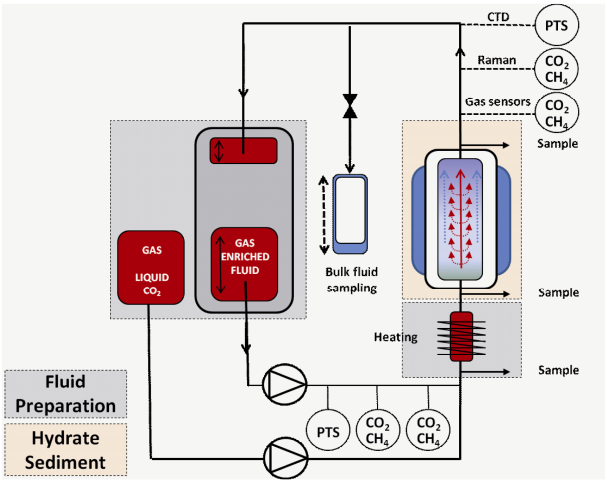

Figure 1: Flow scheme of the experimental high-pressure facility

Pressure vessels and hydraulic components

The high-pressure flow-through system is constructed as a two-stage system (FuE GmbH Fachhochschule Kiel, Kiel , Germany). In the first stage, fluid medium is prepared for injection into the second stage. A 40 L stainless steel high-pressure vessel is used for liquid medium preparation. It is equipped with two flexible volume vessels (1.8 L each) which can be independently filled with a defined water volume at atmospheric pressure, and a defined gas volume is added to reach the respective gas concentration. Magnetic stirrers are used for creating a homogeneous solution of a defined composition. The 40 L vessel is rated for operation at up to 35 MPa and -10 to 150 °C. The vessel is pressurized with a high-pressure pump (Maximator, Zorge, Germany) using water as hydraulic fluid. The second stage is the actual sample incubation stage. Two different high-pressure vessels are used for sample incubation. A cylindrical 2 L stainless steel vessel holding the sample is rated for operation up to 40 MPa and -10 to 120 °C. This sample vessel is equipped with internal containments for the sample to protect the pressure vessels from damage from sediment components. The other vessel is a sapphire tube with a length of 16.5 cm and an inner diameter of 1.2 cm, resulting in a sample volume of 18.7 ml. This vessel is ideally suited for MRI and can be pressurized up to 15 MPa at any temperature between 1 and 10 °C.

The fluids are delivered to the reactors using a Sykam HPLC pump S1122 (Sykam, Fürstenfeldbruck, Germany) for water and gas-enriched water delivery and a TELEDYNE ISCO pump 260D for delivery of gaseous and liquid CO_2. The high-pressure flow-through incubation system is equipped with different high-pressure regulators and valves to control hydraulic pressure and volume flow (SWAGELOK and TESCOM Europe, Selmsdorf, Germany).

Sensor systems, process monitoring and analytical methods

Online CTD and IR gas sensors were supplied by CONTROS Systems and Solutions GmbH (Kiel, Germany). The gas sensors were specifically designed for the experimental purposes. The measurement principle is based on gas diffusion from the process stream over a gas permeable membrane. The buildup of either CO_2 or CH_4 in the measurement chamber is analyzed with IR spectroscopy. The system operation is controlled with a programmable logic controller (PLC). All data are logged via PC.

Further analyses of the fluid composition are done by Raman spectroscopy. During analysis the fluid passes through cells installed both down- and upstream of the reactor. The cells are equipped with sapphire windows, permitting laser light of 125 mW, 532 nm to irradiate the sample inside. Back scattered photons are registered via 1024 x 256 Thermoelectric Open Electrode CCD Detector (HORIBA Jobin Yvon, Longjumeau Cedex, France). Raman analysis was done using a iHR320 spectrometer (HORIBA Jobin Yvon) using a grating of 600 grooves/mm, a macro lens with 40 mm focal length, and spectra accumulation cycling of 2x12 s.

Additional fluid sampling is possible by separating volumes of approx. 10 ml from the overall influent or effluent stream. The pressurized fluids are subsequently decompressed to atmospheric pressure. The partial amounts of water and gas are collected and measured and can then be processed for further solute or gas analysis. The bulk effluent, if not recycled in the process, is collected in gas-tight plastic bags. The bulk sample allows determination of the gas/water ratio and further gas and water analyses.

Although the sensors and the sampling devices of the high-pressure flow-through system allow for a detailed monitoring of the processes inside the reactor, they are all based on volume-integrated quantifications. Local heterogeneities of the transport properties and the availability of reacting species inside the sample vessel cannot be assessed. Magnetic resonance micro imaging (μMRI) is a valuable tool for 3-D visualization of soft condensed matter in a completely non-invasive way [9]. It can provide maps of the fluid phases within the reactor and, at high pressure, also of the gas phases. Nevertheless, this method has rarely been used for pressurized sample systems since the sample container has to be constructed from non-magnetic and electrically non-conducting materials, which excludes the use of metal. This problem has been overcome by designing a reactor, that is based on a sapphire tube hosted in a PEEK housing. An air flow system is used for maintaining the sample at temperatures between 1 and 10 °C. Upstream and downstream sensors and sampling devices are well without the magnetic field of the NMR spectrometer and are identical with those of the stainless steel reactor.

This sample cell can be mounted in a wide-bore 400 MHz NMR spectrometer (Bruker Biospin, Rheinstetten, Germany) which is equipped with a microimaging system. A custom made imaging probe is used, that has an extra large central gap for the feed-through of the cooling air hoses. The diameter of the RF coil is 28 mm and its homogeneous sensitive volume extends about 2 cm in the vertical direction. For a complete image of the sample volume, the reactor is moved to different imaging positions by a stepping motor. The final image is then composed of up to eight sets of 3D or slice data. The spatial resolution of the microimaging systems can be a few tens of micrometers for suitable samples. For time-resolved measurements or samples that exhibit a low basic signal, spatial resolutions of a few hundreds of micrometers are more realistic.

Outline of the experiments

The high-pressure flow-through system described above was tested with both stainless steel reactor and sapphire cell to carry out first hydrate formation, conversion and dissociation experiments. These experiments were essentially focused on testing system functionality and performance for the study purposes. A further aim of this experimental series was the identification of system shortcomings as well as process complications for further experiments and process development in general. In the following an experiment using the 2 L stainless steel reactor is presented. The experiment was performed to obtain first data on CH_4 yields from CH_4-hydrate decomposition and CO_2 retention in the sediment sample using CO_2-rich brines, pure liquefied CO_2 as well as mixtures of CO_2 and water. An additional simple dissolution experiment inside the sapphire reactor was employed to demonstrate the MRI capabilities of our setup during reactions involving gas hydrates in sediments.

RESULTS AND DISCUSSION

CH_4-hydrate preparation

Different methods for preparation of CH_4 hydrates are described in literature. It has been proposed that the most likely pathway for formation of pore filling CH_4 hydrates within marine sediments is by precipitation from oversaturated solutions [11-13]. However, we adapted the ice-seeding method of Stern et al. [14] to accelerate the hydrate formation process while assuring good procedure reproducibility. The artificial sediment was prepared from 300 g of de-ionized water ice and 1350 g of quartz sand. The ice was ground to grains at -20 °C. The experiments described here used the size fraction 0.3-1.0 mm. The reactor was filled with alternating layers of ice grains and pre-cooled quartz sand. To avoid melting of the ice the sediment was kept in liquid nitrogen prior to filling the reactor. The latter was pre-cooled to -8 °C. After closing the vessel multiple pressurization/depressurization cycles with CH_4 gas to a maximum of 1 MPa ensured removal of air and evaporated nitrogen remaining within the sediment pore space. Following the last flushing cycle, injection of CH_4 gas continued until 13 MPa was reached (Figure 2). The gas feeding valves were closed and the pressure measured and recorded with the CTD sensor and the pressure sensor of the HPLC pump. The yield of CH_4-hydrate production was calculated from the pressure decrease. Figure 3 shows the recorded pressure curve and the calculated amount of hydrate being formed in the experiment. Below 0 °C hydrate formation is limited to a thin shell around the ice grains. Further reaction is restricted by molecular diffusion of CH_4 through the solid hydrate shell that separated icy grain cores from free CH_4 gas [14]. After a reaction time of 2 days

the temperature was increased to 2 °C inducing melting of the inner ice grain cores. Density changes due to the melting causes fracturing of the outer hydrate shell, opening up new reaction surfaces for water and CH_4 gas. Hydrate formation is completed after the pressure reaches a stable value at 8.6 MPa.

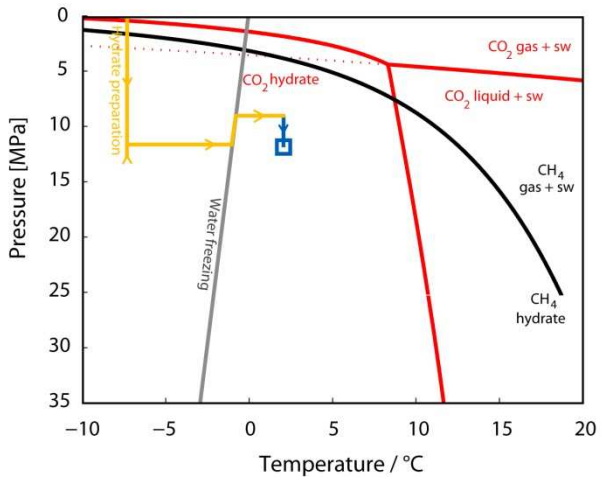

Figure 2: *P*-/*T*-paths followed during CH_4 hydrate formation. The yellow line denotes *P*-/*T*-conditions before injection of water. After hydrate formation was complete the system was flushed and re-pressurized with water to the final pressure of 12 MPa (blue line).

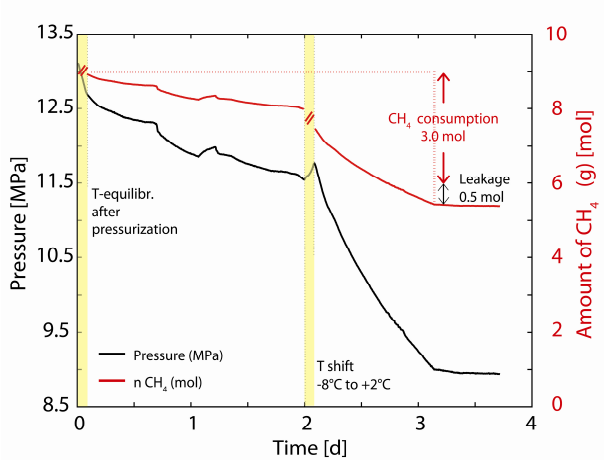

Figure 3: Pressure (black line) and CH_4 gas content (red line) in sample vessel during hydrate formation. After three days a stable pressure plateau is reached indicating full conversion of ice/water to CH_4 hydrate.

CH_4-hydrate dissociation and hydrate conversion

The response of the system to reactive fluid injection was tested in four experimental flow-through sequences: (I) flushing with de-ionized water (1 day), (II) injection of seawater under-saturated with respect to CO_2 (3 days), (III) flushing with de-ionized water (15 days), (IV) injection of a two-phase mixture of liquid CO_2 + CO_2-saturated seawater (5 days). Both, release of CH_4 and retention of CO_2 from/by hydrates were determined from mass balancing based on the composition of the injected and extracted fluids. Figure 4 shows the concentrations of CH_4 and CO_2 in the extracted fluid as determined by Raman spectroscopy.

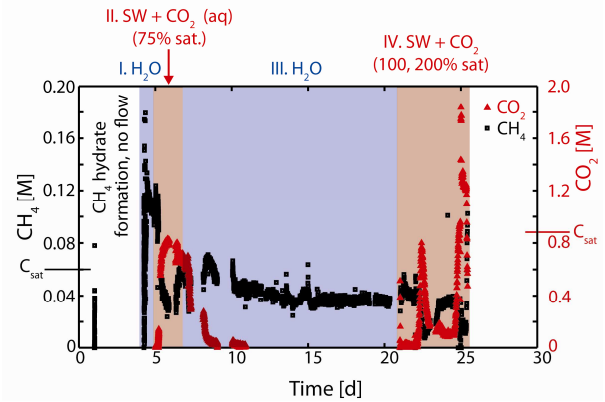

Figure 4: Concentrations of CH_4 (black squares) and CO_2 (red triangles) in the fluid extracted from the sample vessel. Injection sequences (I-IV) are shaded in color. Injection was started on Day 4. Dissolved gas concentrations in seawater in equilibrium with either hydrate species were calculated according to refs. [15] and [16] and are marked by bars at the respective y-intercept of the graph.

The initial flushing was carried out at a flow rate of 10 mL/min to expel excess CH_4 gas from the system and to pressurize to 12 MPa (Figure 2). Figure 4 reveals unsteady concentrations of CH_4 (black) in the extracted fluid with some peak concentrations exceeding the saturation value by a factor of three. The high flow velocity entrained considerable amounts of an additional CH_4 gas phase in the effluent stream, permitting extraction of CH_4 in excess of solubility limits. The presence of free CH_4 gas was verified by analysis of fluid samples. In contrast, low CH_4 concentrations are

indicative of reduced flow velocities of the effluent. Concomitant pressure spikes (not shown) registered in the upstream sensor show that most likely permeability was significantly reduced due to CO_2-hydrate formation in the pore space near the injection point.

The flushing procedure in Sequence I allowed removal of 20% of the excess CH_4 gas. The remainder was retained in pore spaces and is accounted for in the overall mass balance as discussed below. Injection of CO_2 (Sequence II) started with lowering the flow rate to 1 mL/min, causing downstream CH_4 concentrations to drop below saturation. The CO_2 concentration in the injection fluid was adjusted to 0.66 mol/kg. This value corresponds to a saturation of 75% at *P*-/*T*-conditions within the reactor and in equilibrium with CO_2 hydrate and seawater. Maximum downstream CO_2 concentrations peaked around the same value (Figure 4), indicating that none of the CO_2 was retained in the system. Strongly fluctuating concentrations of CH_4 indicate ongoing reaction of injection fluid with CH_4 gas residing in yet untapped domains of sediment. Injection of de-ionized water during Sequence III led to dilution of CO_2. Downstream concentrations decreased accordingly and reached the detection limit on Day 11. Fluctuation of the CH_4 concentration subsided until reaching a steady level near saturation (0.05 mol/L) on Day 15. This shows that CH_4 hydrate formation had ceased. Downstream CH_4 concentrations near saturation reveal that the system was in equilibrium with the effluent solution indicating continuous hydrate dissolution. With the beginning of Sequence IV CO_2-saturated seawater and liquid CO_2 was introduced into the sample vessel. In this period prominent pressure spikes of up to 30 MPa were registered (not shown). The pressure spikes coincide with distinct changes in the extracted fluid composition (Figure 4), suggesting obstruction of fluid pathways followed by sudden sediment fracturing and breakthrough of CO_2-rich liquid. CH_4 concentrations again strongly fluctuated without showing a decreasing trend. The latter indicates that CH_4 hydrate was neither dissociated nor converted into CO_2 hydrate. The experiment was ended on Day 26 after the reduced permeability prohibited further fluid injection.

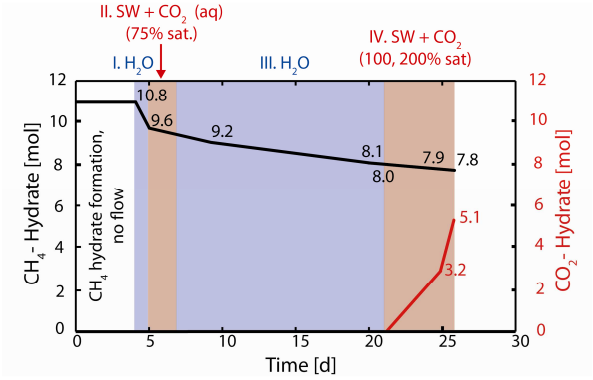

Figure 5: Bulk content of CH_4 and CO_2 in sample vessel as determined from mass balance of injected and extracted fluid. Colors as in Figure 4.

The inventory of CH_4 and CO_2 in the system as determined from mass balance calculations is shown in Figure 5. The figure clearly demonstrates that CH_4 recovery during injection of under-saturated CO_2 solution only marginally differs from pure CH_4 hydrate dissolution (Sequences II + III). The total amount of CH_4 obtained during this 16-day-long period equals only 1.5 mol. Retention of CO_2 in the system begins with the introduction of CO_2 in excess of the solving capacity of the injection fluid in Sequence IV (Figure 5). Clearly immobilization of CO_2 was due to formation of CO_2 hydrate plugs that clog fluid pathways causing the observed pressure spikes and sediment fracturing.

Recovery of the sample revealed retention of the layered sediment column as pre-determined from inter-bedding ice grains and quartz sand during sample preparation (see Section "CH_4-hydrate preparation" & Figure 6). Spatial Raman analysis exposed the presence of both CH_4 hydrate and CO_2 hydrate. All remaining CH_4 hydrate formed isolated, granular domains embedded in the pre-determined layers of ice within the sediment column. CO_2 hydrate was exclusively found in the pore space of the quartz sand matrix. CO_2 hydrate distribution showed a strong preference towards lower parts of the sediment column, near the injection site. This lends further support to the hypothesis of immediate CO_2 hydrate precipitation after injection of CO_2 in excess of solubility during the last injection sequence.

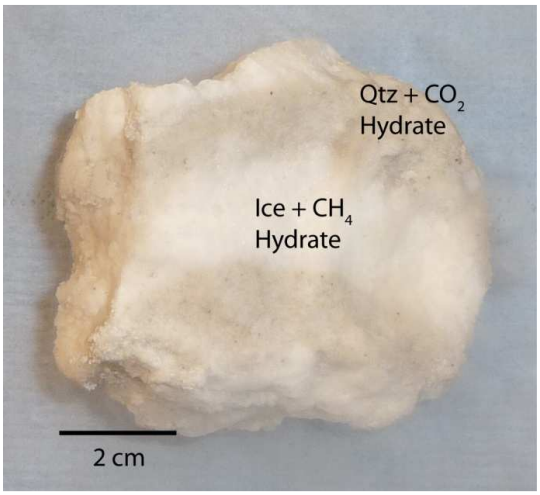

Figure 6: Hydrate piece recovered from the sample vessel after the end of the flow-through experiment. The initial layered structure of the sediment column with alternating layers of quartz sand and ice is still clearly visible

Two important results can be derived from this first flow-through experiment:

1. Aqueous, CO_2-rich solutions injected into permeable, CH_4 hydrate-bearing sediment do not trigger CH_4 hydrate conversion nor significant CH_4 hydrate destabilization, if CO_2 concentrations are below saturation concentrations. Hence, the results suggest that injection of CO_2 in fluids under-saturated with respect to CO_2 is not a viable option, not for CO_2 storage in hydrates nor for CH_4 recovery.
2. Injection of super-saturated CO_2-rich brines into water-saturated sediments causes immediate precipitation of CO_2 hydrate. This effectively reduces permeability and quickly obstructs fluid pathways around the injection site. This not only impedes process performance for both CH_4 recovery and large-scale CO_2 storage. Continued injection also results in quickly rising reservoir pressures, potentially jeopardizing cap rock integrity.

Different possibilities to overcome the technological problems and to increase CH_4 hydrate conversion and CH_4 release are currently tested. This includes the injection of liquid CO_2 under water-limited conditions, additional heat injection by using supercritical CO_2 or methods to pre-condition the sediment by temperature or pressure adjustment.

Tracking hydrate dissolution via µMRI

The sapphire reactor was filled with a mixture of quartz sand and C_3H_8/ CH_4 mixed gas hydrate. Although we chose to work with a relatively stable hydrate system, some decomposition took place during the mounting and pressurization of the sample cell. The system was brought into the hydrate stability field by pressurization to 3 MPa with de-ionized water. At this point, imaging was started. The imaging sequence used was a multi-slice spin-echo sequence with a repetition time of TR = 1000 ms, an echo time of TE = 3.1 ms, a slice thickness of 0.5 mm, 25 slices, an in-plane field of view of 3 x 1.5 cm^2 and an in-plane resolution of 0.23 mm. Figure 7a shows the central slice through the sample which has been assembled from 6 individual images. It can be seen that the dark sand matrix is fractured and contains fluid filled cavities, which show up as bright areas in the image. Obviously, gas from the dissociating gas hydrates formed those voids within the sediment. Additionally, pressure spikes that occurred during pressurization might also have fractured the sediment matrix.

As a next step, a constant flow of de-ionized water with a flow rate of 2 ml/min was imposed on the system, which was operated at a temperature of 6 °C and a mean pressure of 7.5 MPa. Imaging was performed continuously over 1 h 55 min with a complete set of images measured every 8.5 min. During that time, the gas hydrate dissolved in the CH_4 under-saturated water and the sand matrix was destabilized and settled at the bottom of the sample cell. This process can clearly been followed in the images shown in Figure 7, which demonstrates the strength and ability of the applied imaging method.

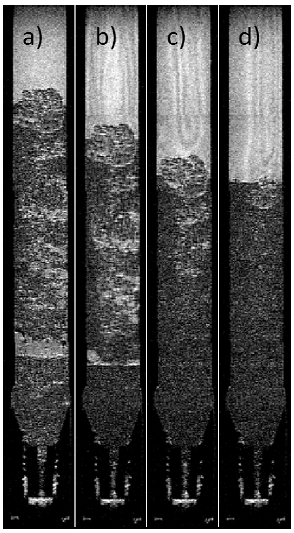

Figure 7: Time series of NMR images of a hydrate sand mixture during hydrate dissociation (see text for detailed information). a) without flow; b-d) flow of 2 ml/min; time between images: 17 min.

CONCLUSIONS

A novel experimental high-pressure flow-through system was designed and constructed to assess the feasibility of recovering CH_4 from gas hydrate-bearing marine sediments via injection of CO_2. The system consists of a versatile fluid conditioning and delivery unit which can be equipped with a variety of reactors and analytical instruments. Characteristic feature of the experimental design is the possibility to monitor and log process parameters on-line and non-invasively, while pressurized fluids are being pumped through the sediment sample at simulated in-situ conditions.

The efficiency of the facility was tested in two experimental set-ups using a 2 L stainless steel pressure reactor in the first run and a 15 mL sapphire tube in the second. Experimental results obtained with the former suggest that injection of CO_2 in both under-saturated and supersaturated aqueous solutions are inadequate means for CH_4 recovery from and large-scale storage of CO_2 within hydrate-bearing marine sediments. MRI in connection with a pressurized sapphire sample vessel proved to be a powerful tool for non-invasive mapping of processes within the sediment occurring on the µm-scale.

Our experiments expectedly disclose the complex response of a multiphase system such as marine sediments to CO_2-rich fluid injection. They thereby exemplify the necessity of approaching this issue via integration of several analytical techniques in a single approach. Results from our experiments will help to identify suitable CO_2 injection and CH_4 hydrate exploitation scenarios and contribute to the understanding of natural hydrates as well as flow dynamics in hydrate-bearing sediments on different scales.

ACKNOWLEDGMENTS

This work was conducted within the German gas hydrate initiative SUGAR funded by the German Ministry of economy (BMWi) under grant no. 03SX250 and the CLATHRAT project funded by RWE DEA AG and Wintershall Holding AG.

REFERENCES

[1] Hirohama S, Shimoyama Y,Wakabayashi A, Tatsuta S, Nishida N. *Conversion of CH_4-hydrate to CO_2-hydrate in liquid CO_2.* J. Chem. Eng. Jpn. 1996;29(6):1014-1020

[2] Komai T, Yamamoto Y, Ohga K. *Dynamics of reformation and replacement of CO_2 and CH_4 gas hydrates*. Ann. N. Y. Acad. Sci. 2000;912:272-280.

[3] Yoon JH et al. *Transformation of methane hydrate to carbon dioxide hydrate: In situ Raman spectroscopic observations*. J. Phys. Chem. A. 2004;108(23):5057-5059.

[4] Ota M, Abe Y, Watanabe M, Smith Jr RL, Inomata H. *Methane recovery from methane hydrate using pressurized CO_2*. Fluid Phase Equilib. 2005a;228-229:553-559.

[5] Ota M, Morohashi K, Abe Y, Watanabe M, Smith Jr RL, Inomata H. *Replacement of CH_4 in the hydrate by use of liquid CO_2*. Energy Convers. Manage. 2005b;46(11-12):1680-1691.

[6] Park Y, Kim DY, Lee JW, Huh DG, Park KP, Lee J, Lee H. *Sequestering carbon dioxide into complex structures of naturally occurring gas hydrates.* PNAS. 2006;103(34):12690-12694.

[7] Ota M, Saito T, Aida T, Watanabe M, Sato Y, Smith Jr RL, Inomata H. *Macro and microscopic CH_4-CO_2 replacement in CH_4 hydrate under pressurized CO_2.* AIChE J. 2007;53(10):2715-2721.

[8] Zhou XT, et al. *Replacement of methane from quartz-bearing hydrate with carbon dioxide-in-water emulsion*. Energy Fuels. 2008;22(3):1759-1764.

[9] Ersland G, Husebo J, Graue A, Baldwin BA, Howard J, Stevens J. *Measuring gas hydrate formation and exchange with CO_2 in Bentheim*

sandstone using MRI tomography. Chem. Eng. J. 2010;158(1):25-31.
[10] Schicks JM, Spangenberg E, Giese R, Steinhauer B, Klump J, Luzi M. *New Approaches for the Production of Hydrocarbons from Hydrate bearing Sediments*. Energies. 2011;4:151-172.
[11] Hyndman RD, Davis EE. *A mechanism for the formation of methane hydrate and sea floor bottom-simulating reflectors by vertical fluid expulsion.* J. Geophys. Res. 1992;97:7025-7041.
[12] Buffett BA, Zatsepina OY. *Formation of gas hydrate from dissolved gas in natural porous media*. Mar. Geol. 2000;164:69-77.
[13] Spangenberg E, Kulenkampff J, Naumann R, Erzinger J. *Pore space hydrate formation in a glass bead sample from methane dissolved in water*. Geophys. Res. Lett. 2005;32:1-4.
[14] Stern LA, Kirby SH, Durham WB. *Polycrystalline methane hydrate: Synthesis from superheated ice, and low temperature mechanical properties*. Energy Fuels. 1998;12:201–211.
[15] Tishchenko P, Hensen C, Wallmann K, Wong CS. *Calculation of the stability and solubility of methane hydrate in seawater*. Chem. Geol. 2005;219(1-4):37-52.
[16] Tishchenko P., Wong C.S., Johnson W. K., Haeckel M., Wallmann K., Aloisi G., Stability and solubility of CO_2 hydrate in seawater. 8th International Carbon Dioxide Conference (ICDC8), Jena, Germany, 13-19 September 2009.